ferent types of experiments were performed by Reinkober to establish the two sets of E and G values Young's modulus E was found by measuring elongations of the fibers subject to static loads; torsion modulus G was found by measuring the frequency of a torsion pendulum in which the test fiber provided the torsion spring Thus, a systematic discrepancy between the two sets could conceivably arise

Conclusions

The foregoing analysis of a limited set of experimental data tends to substantiate a hypothesis that the remarkable physical properties of thin glass fibers are associated with a skin layer of modified structure, posssibly exhibiting properties similar to those found in crystalline modifications of the same material Such a mechanism, if found effective in refractory materials capable of forming glassy compounds, would enhance the utility of glass-fiber-forming processes in the refractory materials field

References

[1] Griffith, A A, "The phenomena of ruptuie and flow in solids," Phil Trans Roy Soc London **221**, 163–198 (1920)
[2] Jurkov, S, 'Effect of increased strength of thin filaments,' Tech Phys USSR **I**, 386–399 (1935)
[3] Beams, T W, "Mechanical strength of thin films of metals," Phys Rev **100**, 1657–1661 (1955)
[4] Brenner, S S, "Tensile strength of whiskers," J Appl Phys **27**, 1484–1491 (1956)
[5] Shanley, F R, "On the strength of fine wires," Rand Corp Paper P-1654 (April 1, 1959)
[6] Otto, W H, "Relationship of tensile strength of glass fibers to diameter,' J Am Ceram Soc **38**, 122–124 (1955)
[7] Reinkober, O, 'Elasticity and strength in thin quartz-filaments," Physik **33**, 32 (1932)

Calculation of the Surface Range of a Ballistic Missile

P R Escobal*
Operations Research Inc, Santa Monica, Calif

A TECHNIQUE is developed which enables calculation of the distance between two points constrained to lie on the surface of an arbitrary ellipsoid The quadratic forms involved in the geometry are transformed in such a manner that integration of arc length may be computed by means of normal elliptical integrals of the second kind

Usually surface range is calculated on the surface of a sphere by the relation $s = r\theta$ where r = radius of sphere, and θ = subtended central angle (in radians) This range is, in effect, a great circle arc in a plane which passes through the geometrical center of the sphere The purpose of this note is to describe a technique for obtaining the arc range on the surface of an ellipsoid It is assumed that the definition of distance is taken to be the intersection of the given ellipsoid with a plane which passes through the geometrical center of the ellipsoid

When the burnout and impact subvehicle longitude and geocentric latitude of a missile are known,† denoted, respectively, by λ_{EB}, ϕ_B, and λ_{EI}, ϕ_I, the calculation of surface range can be accomplished in the following manner The coordinates of the burnout and impact points are given by

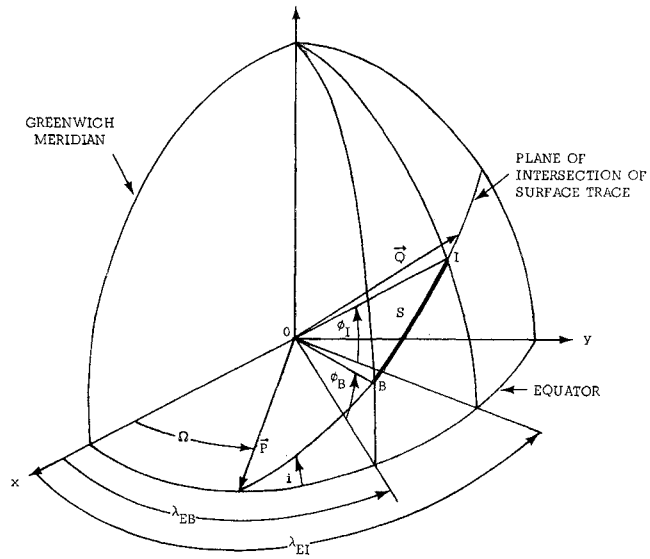

Fig 1 Coordinate system

$$\begin{aligned} x_B &= r_B \cos\phi_B \cos\lambda_{EB} & x_I &= r_I \cos\phi_I \cos\lambda_{EI} \\ y_B &= r_B \cos\phi_B \sin\lambda_{EB} & y_I &= r_I \cos\phi_I \sin\lambda_{EI} \\ z_B &= r_B \sin\phi_B & z_I &= r_I \sin\phi_I \end{aligned} \tag{1}$$

Thus, the equation of plane BOI in Fig 1 is given at once by

$$\begin{vmatrix} x & y & z & 1 \\ x_B & y_B & z_B & 1 \\ x_I & y_I & z_I & 1 \\ 0 & 0 & 0 & 1 \end{vmatrix} = 0 \tag{2}$$

Letting the coefficients A, B, C be defined by Eq (2), it is possible to write

$$Ax + By + Cz = 0 \tag{3}$$

where

$$\begin{aligned} A &= y_B z_I - y_I z_B \\ B &= x_I z_B - x_B z_I \\ C &= x_B y_I - x_I y_B \end{aligned}$$

The equation of an ellipsoid can be written as

$$(x^2/a^2) + (y^2/b^2) + (z^2/c^2) = 1 \tag{4}$$

where a is the semimajor axis and c is the semiminor axis of the international ellipsoid Usually $a = b$, and an oblate spheriod is taken as the model of the earth The analysis, however, is not restricted to this case In canonical units a is usually taken to be unity, and c can be calculated from the relation

$$c = a(1 - f) \tag{5}$$

where f is the flattening which is taken to be 1/298 3

By defining the unit vectors $\mathbf{P}$ and $\mathbf{Q}$, ($\mathbf{P} \perp \mathbf{Q}$) (see Fig 1)

$$\begin{aligned} P_x &= \cos\Omega & Q_x &= -\sin\Omega \cos i \\ P_y &= \sin\Omega & Q_y &= \cos\Omega \cos i \\ P_z &= 0 & Q &= \sin i \end{aligned} \tag{6}$$

where the orientation angles Ω and i are obtained from Ref 1 as

Received December 12, 1963 This work was supported by the Special Projects Office, Department of the Navy, under Contract No NOw 61-0145
* Consultant Member AIAA
† The burnout and impact points are just two given arbitrary points It would be correct to insert the coordinates of New York and Paris and thus obtain the distance between the two cities

$$\begin{aligned} \cos i &= C/R & \cos i &= C/R \\ \cos\Omega &= -\frac{B}{[A^2+B^2]^{1/2}} & \cos\Omega &= \frac{B}{[A^2+B^2]^{1/2}} \\ \sin\Omega &= \frac{A}{[A^2+B^2]^{1/2}} & \sin\Omega &= \frac{A}{[A^2+B^2]^{1/2}} \end{aligned} \quad (7)$$

with the left equations holding for $i \leq \pi/2$ and the right equations holding for $i > \pi/2$ and

$$R = [A^2 + B^2 + C^2]^{1/2}$$

it is possible to map points in xyz space (Fig 1) into points in the plane *BOI* by the equations

$$\begin{aligned} x &= P_x x_\omega + Q_x y_\omega \\ y &= P_y x_\omega + Q_y y_\omega \\ z &= P x_\omega + Q_z y_\omega \end{aligned} \quad (8)$$

Upon substitution of these equations into Eq (4), it is evident that

$$\omega_1 x_\omega^2 + \omega_2 y_\omega^2 + \omega_3 x_\omega \omega_\omega = 1 \quad (9)$$

where

$$\begin{aligned} \omega_1 &= (P_x^2/a^2 + P_y^2/b^2) \\ \omega_2 &= (Q_x^2/a^2 + Q_y^2/b^2 + Q^2/c^2) \\ \omega_3 &= 2(P_x Q_x/a^2 + P_y Q_y/b^2) \end{aligned}$$

If $a = b$, then it is easy to verify that

$$\begin{aligned} \omega_1 &= \frac{1}{a^2}(1 - P^2) = \frac{1}{a^2} \\ \omega_2 &= \frac{1}{a^2} + \left(\frac{1}{c^2} - \frac{1}{a^2}\right) Q^2 \\ \omega_3 &= 0 \end{aligned}$$

Furthermore, from examination of these equations, the following inequality can be written:

$$\omega_2 > \omega_1 > \omega_3 = 0$$

In order to integrate easily for the arc length along Eq (9), it will be necessary to make the last term of Eq (9) vanish In effect, a rotation will now be made in the plane *BOI* by means of rotation equations:

$$\begin{aligned} x_\omega &= x_h \cos\eta - y_h \sin\eta \\ y_\omega &= x_h \sin\eta + y_h \cos\eta \end{aligned} \quad (10)$$

Substitution of these equations into Eq (9) produces

$$\begin{aligned} &(\omega_1 \cos^2\eta + \omega_2 \sin^2\eta + \omega_3 \cos\eta \sin\eta) x_h^2 + \\ &\quad (\omega_1 \sin^2\eta + \omega_2 \cos^2\eta - \omega_3 \cos\eta \sin\eta) y_h^2 + \\ &\quad [(\omega_2 - \omega_1) \sin 2\eta + \omega_3 \cos 2\eta] x_h y_h = 1 \end{aligned} \quad (11)$$

It follows that by choosing

$$\eta = \tfrac{1}{2} \tan^{-1}[\omega_3/(\omega_1 - \omega_2)] \quad (12)$$

Eq (9) transforms to

$$\xi_1 x_h^2 + \xi_2 y_h^2 = 1 \quad (13)$$

where

$$\begin{aligned} \xi_1 &= \omega_1 \cos^2\eta + \omega_2 \sin^2\eta + \omega_3 \cos\eta \sin\eta \\ \xi_2 &= \omega_1 \sin^2\eta + \omega_2 \cos^2\eta - \omega_3 \cos\eta \sin\eta \end{aligned} \quad (14)$$

It should be noted that the first rotation maps the end points into the plane *BOI* by the equations

$$\begin{aligned} x_\omega &= x P_x + y P_y \\ y_\omega &= x Q_x + y Q_y + z Q \end{aligned} \quad (15)$$

and that the second rotation, effected in order to eliminate the cross product term, maps points in the *BOI* plane into new points within the plane by

$$\begin{aligned} x_h &= x_\omega \cos\eta + y_\omega \sin\eta \\ y_h &= y_\omega \cos\eta - x_\omega \sin\eta \end{aligned} \quad (16)$$

Now, since Eq (13) must also be an ellipse, it is clear that the transformed equation can be written in standard form as

$$\frac{x_h^2}{F^2} + \frac{y_h^2}{G^2} = 1 \qquad \xi_1 = \frac{1}{F^2} > 0 \qquad \xi_2 = \frac{1}{G^2} > 0 \quad (17)$$

Solving for y_h and differentiating, there results

$$\left(\frac{dy_h}{dx_h}\right)^2 = \left(\frac{\xi_1^2}{\xi_2}\right) \frac{x_h^2}{1 - \xi_1 x_h^2} \quad (18)$$

Using the definition of arc length, i e ,

$$S = \int_{y_{hB}}^{y_{hI}} \left[1 + \left(\frac{dx_h}{dy_h}\right)^2\right]^{1/2} dy_h = \int_{x_{hB}}^{x_{hI}} \left[1 + \left(\frac{dy_h}{dx_h}\right)^2\right]^{1/2} dx_h \quad (19)$$

and substituting the value of the rate of change of y_h with respect to x_h, it is possible to write

$$S = \int_{x_{hB}}^{x_{hI}} \left[\frac{1 + (\xi_1^2/\xi_2 - \xi_1) x_h^2}{1 - \xi_1 x_h^2}\right]^{1/2} dx_h \quad (20)$$

Introducing the parameter w, the integral transforms to‡

$$S = \frac{1}{(\xi_1)^{1/2}} \int_{w_i}^{w_2} \left[\frac{1 - (1 - \xi_1/\xi_2) w^2}{1 - w^2}\right]^{1/2} dw \quad (21)$$

with $w = (\xi_1)^{1/2} x_h$ Rewriting the integral as

$$\begin{aligned} S = &\frac{1}{(\xi_1)^{1/2}} \int_0^{w_2} \left[\frac{1 - (1 - \xi_1/\xi_2) w^2}{1 - w^2}\right]^{1/2} dw - \\ &\frac{1}{(\xi_1)^{1/2}} \int_0^{w_1} \left[\frac{1 - (1 - \xi_1/\xi_2) w^2}{1 - w^2}\right]^{1/2} dw \end{aligned} \quad (22)$$

and letting

$$\begin{aligned} \theta_1 &= \sin^{-1} w_1 \\ \theta_2 &= \sin^{-1} w_2 \qquad -\pi/2 \leq (\theta_1, \theta_2) \leq \pi/2 \\ k^2 &= (1 - \xi_1/\xi_2) < 1 \end{aligned} \quad (23)$$

the integration is accomplished by the use of the normal elliptic integral of the second kind[2] as

$$S = 1/(\xi_1)^{1/2} \{E(\theta_2, k) - E(\theta_1, k)\} \quad (24)$$

where $\xi_1 > 0$ by Eq (17) It should be noted that for the case $a = b$, the θ_i of Eq (24) are the angles between the projection of the $y_{\omega i}$ axis on the equator plane and the semimajor axis a

Computational Procedure

Given r_B, λ_{EB}, ϕ_B, and r_I, λ_{EI}, ϕ_I, compute x_B, y_B, z_B, and x_I, y_I, z_I by means of Eqs (1) Obtain A, B, C from Eq (3) and the unit vectors P_x, P_y, Q_x, Q_y, and Q from Eqs. (6) and (7) Calculate x_ω and y_ω from Eqs (10) for both burnout and impact Compute ω_1, ω_2, and ω_3 from Eq (9), and if $\omega_3 \neq 0$, obtain the rotation angle η from Eq (12) Now obtain for burnout and impact points x_h and y_h from Eqs (16) Note that these parameters will be equal to x_ω and y_ω if $\omega_3 = 0$ Calculate ξ_1 by means of Eq (14) Obtain limits at burnout (w_1) and impact (w_2) by Eq (21), and k^2, θ_1, and θ_2 from Eq (23) Evaluate $E(\theta_2, k)$, $E(\theta_1, k)$ and compute the surface range from Eq (24) Note that if

‡ If $\xi_1 > \xi_2$, then replace ξ_1 by ξ_2 and take $w = (\xi_2)^{1/2} y_h$ in Eq (21) This will not happen for the case $a = b$

canonical units have been used, the value of the arc length or surface range between the two given points is given in earth radii

References

[1] Moulton, F R, *An Introduction to Celestial Mechanics* (The Macmillan Company, New York, 1914), p 146

[2] Davis, H T, *Introduction to Nonlinear Differential and Integral Equations* (Dover Publications, Inc, New York, 1962), p 145

Correlation of Flat-Plate Pressures Using the Rarefaction Parameter $M_\infty C_\infty^{1/2}/Re_{x_\infty}^{1/2}$

H Eugene Deskins*

ARO, Inc, Arnold Air Force Station, Tenn

Experimental flat-plate pressure data with apparent slip effects are presented A departure of $(\Delta p/p_\infty)/\bar{\chi}_\infty$ from the continuum flow constant value (γ = const, T_w/T_0 = const), which signifies the apparent onset of slip-flow effects, is shown to occur when $M_\infty C_\infty^{1/2}/Re_{x_\infty}^{1/2} \approx 0\,1$ to $0\,2$ The departure point appears to be independent of wall heating

RECENTLY, Talbot[1] showed the low-speed slip-flow parameter $M_\infty/\bar{R}e_{x_\infty}^{1/2}$ to be applicable to the hypersonic regime when $\bar{R}e_{x_\infty} = (\rho_\infty U_\infty X)/(\mu_\infty C_\infty)$, where $C_\infty = (\mu T_\infty)/(\mu_\infty T)$ He suggested that this parameter would be appropriate for correlation of experimental data in slip flow and pointed out that slip effects on surface pressure have been observed when $M_\infty C_\infty^{1/2}/Re_{x_\infty}^{1/2} \geq 0\,10$ The purpose of this note is to present additional cold-wall, sharp, flat-plate pressure data in support of Talbot's observation and analysis

The experimental data presented in this note were obtained from recent tests in the Arnold Engineering Development Center 50-in hotshot tunnel[2] and the continuous-flow, low-density hypersonic tunnel (LDH)[3] at cold-wall conditions ($T_w/T_0 \simeq 0\,1$) and from tests, reported by Aroesty,[4] in the University of California low-density wind tunnel (LDWT) at a hot-wall condition ($T_w/T_0 \simeq 1\,0$) Most of the data of Nagamatsu et al[5] pertain completely to slip flow, and, therefore, deviation from continuum flow could not be observed; these data are not included

Strong viscous interaction theory[6] specifies that the induced pressure be a linear function of the viscous interaction parameter $\bar{\chi}_\infty$, where $\bar{\chi}_\infty = M_\infty^3/\bar{R}e_{x_\infty}^{1/2}$ The slope of the function in continuum flow is only dependent on the ratio of specific heats γ and the wall to total temperature ratio (T_w/T_0), e g, $m(\gamma, T_w/T_0) = (\Delta p/p_\infty)/\bar{\chi}_\infty$ The data are presented in terms of these parameters in Fig 1 When $\bar{\chi}_\infty$ is less than about 40, the hotshot experimental data support the linear relationship Two sets of data are plotted, one for a very sharp leading edge, $d = 0\,001$ in, and one for a slightly more blunt leading edge, $d = 0\,01$ in There is no difference (within the data scatter) in these data, which indicates that bluntness effects are completely overcome by the viscous-induced pressure Of particular interest is the divergence from a linear relationship as $\bar{\chi}_\infty$ increases

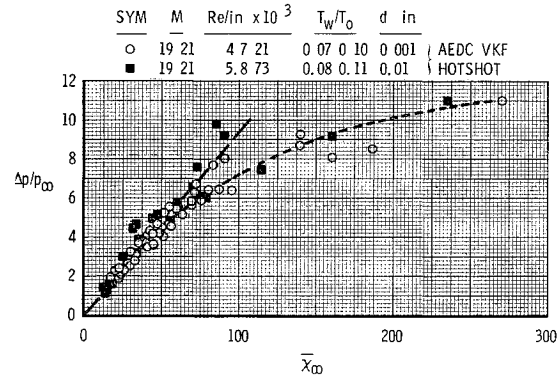

Fig 1 Sharp flat-plate pressure distribution

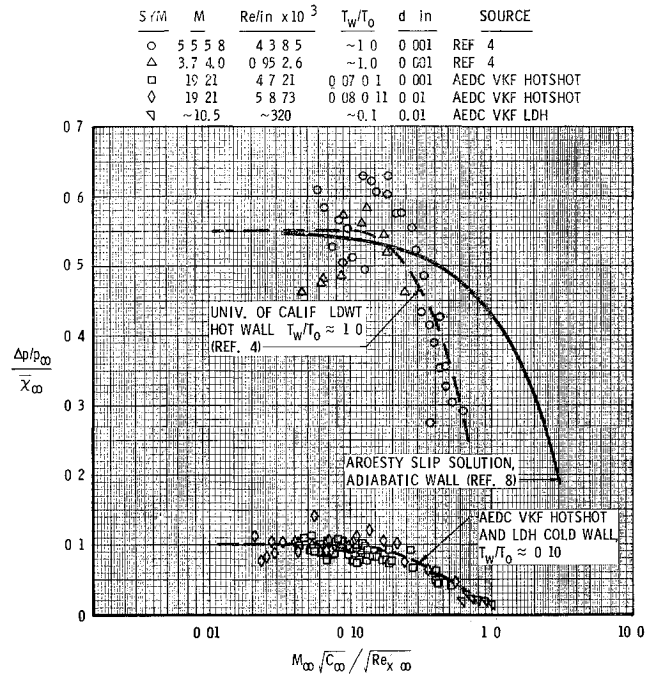

Fig 2 Effect of slip flow, pressure distribution

This is brought out in Fig 2, which shows Aroesty's data[4] and the present experimental data plotted in terms of $(\Delta p/p_\infty)/\bar{\chi}_\infty$ and Talbot's slip parameter There is large scatter inherent in this type of figure, but it does not obscure nor alter the results For continuum flow, the ratio $(\Delta p/p_\infty)$ to $\bar{\chi}_\infty$ is independent of the slip parameter, whereas as slip effects are encountered it decreases with increasing slip parameter Both the hot-wall and the cold-wall data indicate the onset of slip effects at about $M_\infty C_\infty^{1/2}/Re_{x_\infty}^{1/2} \simeq 0\,10$ to $0\,20$ This is in excellent agreement with the observations of Talbot[1] and illustrates the dependence of slope on the slip parameter Vidal et al[7] observed a similar trend in their studies in the Cornell shock tunnel The initial departure from the continuum constant value appears to be independent of wall temperature, which is in agreement with Talbot Included is the Aroesty[8] solution of strong interactions with slip boundary conditions Although the theory is not adequate to predict quantitatively the slip effect, it does predict the correct trend, thus giving support to the use of the rarefaction parameter $M_\infty C_\infty^{1/2}/Re_{x_\infty}^{1/2}$

Received December 19, 1963 This work was sponsored by the Arnold Engineering Development Center, Air Force Systems Command, U S Air Force, under Contract No AF 40(600)1000

* Project Engineer, Hypervelocity Branch, von Kármán Gas Dynamics Facility

References

[1] Talbot, L, "Criterion for slip near the leading edge of a flat plate in hypersonic flow," AIAA J 1, 1169–1171 (1963)

[2] "Test facilities handbook," 4th ed, Vol 4, von Kármán Gas Dynamics Facility, Arnold Eng Dev Center (July 1962)